Multipeak Kondo Effect in One- and Two-Electron Quantum Dots

A. Vidan, M. Stopa, and R. M. Westervelt
Division of Engineering and Applied Sciences and Department of Physics, Harvard University, Cambridge, Massachusetts 02138, USA

M. Hanson and A. C. Gossard
Materials Department, University of California, Santa Barbara, California 93106, USA
(Received 20 November 2005; published 17 April 2006)

We have fabricated a few-electron quantum dot that can be tuned down to zero electrons while maintaining strong coupling to the leads. Using a nearby quantum point contact as a charge sensor, we can determine the absolute number of electrons in the quantum dot. We find several sharp peaks in the differential conductance, occurring at both zero and finite source-drain bias, for the one- and two-electron quantum dot. We attribute the peaks at finite bias to a Kondo effect through excited states of the quantum dot and investigate the magnetic field dependence of these Kondo resonances.

DOI: 10.1103/PhysRevLett.96.156802 PACS numbers: 73.63.Kv, 72.15.Qm, 73.21.La, 73.23.−b

The Kondo effect arises when the degenerate or nearly degenerate states of an isolated electron system, which are not coupled through any direct interaction, acquire an effective coupling, and thereby hybridize, via the virtual exchange of electrons with one or more neighboring Fermi surfaces [1]. The simplicity of the conditions demanded by the Kondo effect contributes to its ubiquity in electron systems as well as to the variety of phenomena that are distinct manifestations of Kondo physics. The initial experimental puzzle which required the Kondo effect for its elucidation concerned the diverging resistivity of metals doped, intentionally or otherwise, with $3d$ transition metal impurities possessing a local magnetic moment [2]. By contrast to the case of impurities in metal, however, the observation of Kondo physics in semiconductor quantum dots, which are artificial atoms whose coupling, spin, and energy parameters are subject to delicate control [3], dramatically widened the classes of Kondo behavior which could be observed and explained [4–9].

Nonlinear measurements of transport through Coulomb blockaded quantum dots have become a standard method for investigating the excited states of dot electrons. Frequently observed inelastic cotunneling lines in Coulomb diamonds [10] are a signature of a virtual exchange of electrons with two Fermi surfaces (the leads) which produce a preferential electron flow from source to drain. This phenomenon is, at least, the lowest order fundamental process from which arises the Kondo effect. In this Letter, we present results of transport measurements through a single quantum dot occupied by one or two electrons ($N = 1$ or 2) which, in both cases, exhibit sharp peaks in the differential conductance beyond the linear regime. Analysis of the temperature dependence and the peak splitting due to a magnetic field indicate that these cotunneling lines represent the fully coherent Kondo effect. We analyze the revealed level spacing in terms of a disordered, quasi-1D structure of the dot and indicate that the unusually low-energy excitations are an expected characteristic of such systems, and we note that similar features in transport through 1D nanotube devices have already been observed [11].

We define the quantum dot using six Cr:Au surface gates and a 30 nm deep ion-etched trench on a modulation doped $GaAs/Al_{0.3}Ga_{0.7}As$ heterostructure containing a two-dimensional electron gas (2DEG) 52 nm below the surface. Low temperature Hall measurements determined the 2DEG sheet density $n_s = 3.8 \times 10^{11}$ cm^{-2} and mobility $\mu = 460\,000$ cm^2 V^{-1} s^{-1}. A scanning electron micrograph of the device is shown in Fig. 1(a). The device was cooled in a ^{3}He-^{4}He dilution refrigerator, and the differential conductance through the quantum dot was measured between leads I and II by adding a small ac excitation voltage to a dc source-drain bias V_{SD} and recording the current with a current preamplifier and lock-in amplifier. A large negative voltage was placed on gate G6 to suppress any tunneling through the third terminal. All measurements, except those in Fig. 3(a), were performed at the base temperature of 40 mK. Figures 1(b) and 1(c) show typical Coulomb blockade conductance oscillations and Coulomb diamonds for the quantum dot in the few-electron regime. Our geometry allows us to tune the number of electrons in the quantum dot from approximately 20 electrons down to zero electrons. Furthermore, we observe clear signatures of a shell structure [12] in the quantum dot, including an alternation in the Coulomb blockade peak heights for the first few electrons entering the dot, different areas for each Coulomb diamond, and odd-even signatures at zero source-drain bias.

By placing a large negative voltage on both gates G5 and G6, we can reduce the size of the quantum dot. Self-consistent electronic structure simulations of the full three-dimensional structure of our dot, including wafer profile, donor layer disorder, and the device surface gate pattern, show that the potential profile for the 2DEG electrons can become long and narrow [Fig. 2(a)]. Our device has a nearby gate G7 that forms a quantum point contact

 © 2006 The American Physical Society

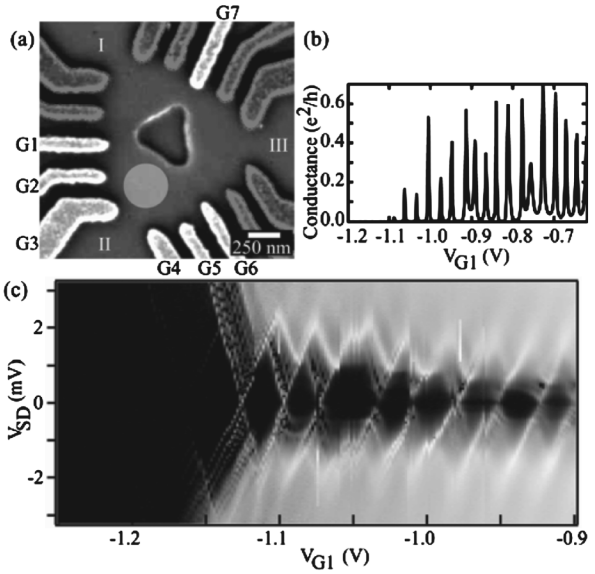

FIG. 1. (a) Scanning electron micrograph of the quantum dot device. Light gray regions are Cr : Au surface gates. Only the highlighted gates are used in these measurements. The center region is a 30 nm deep ion-etched trench. (b) Coulomb blockade oscillations as a function of side gate voltage V_{G1}. (c) Gray-scale plot of the differential conductance dI/dV_{SD}. Light regions correspond to enhanced conductance.

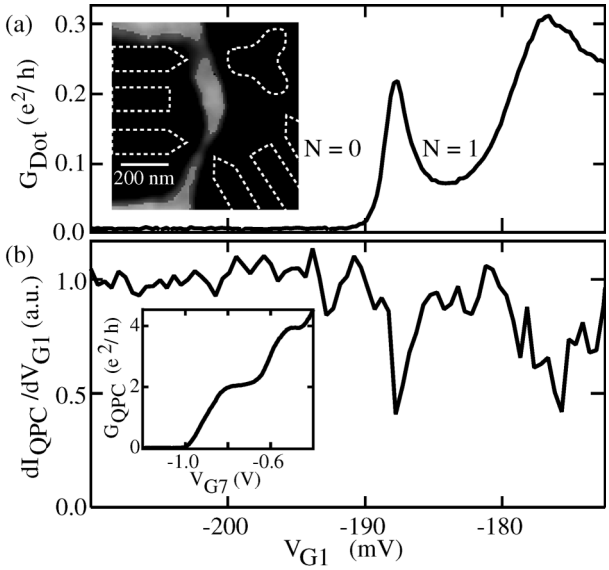

FIG. 2. (a) Coulomb blockade conductance of the quantum dot, when tuned down to the one- and two-electron regime. Inset: Potential profile from a self-consistent electronic structure simulation showing the resulting quasi-1D shape of the quantum dot. The center of the dot (light gray region) is at ~ -4 meV relative to the Fermi level of the 2DEG, with QPC barrier heights of $\sim$4 meV. (b) Simultaneously measured differential conductance dI_{QPC}/dV_{G1} through a nearby QPC biased below the first conductance plateau. The QPC acts as a charge sensor, showing a drop in dI_{QPC}/dV_{G1} as the number of electrons on the dot changes. The absence of additional dips reveals the absolute number of electrons on the dot, starting at $N = 0$. Inset: Quantized conductance of the QPC.

(QPC) against the center etched trench. Measuring the conductance through leads I and III, we find that the quantum point contact shows clear conductance plateaus, as shown in the inset of Fig. 2(b). Biasing the point contact below the first conductance plateau, where the slope is the steepest, allows it to act as a very sensitive charge sensor for the quantum dot [13]. As the quantum dot goes through a Coulomb blockade peak, a sharp decrease in the point contact conductance dI_{QPC}/dV_{G1} is observed. Figures 2(a) and 2(b) show the conductance through the quantum dot and dI_{QPC}/dV_{G1} measured simultaneously. The absence of further Coulomb blockade oscillations in the quantum dot conductance or dips in the point contact conductance as V_{G1} is made more negative indicates that the quantum dot is empty of electrons. In the rest of the measurements presented here, G7 is turned off and lead III is left floating.

In most quantum dots, as the size is reduced using the side gates, the large negative voltage applied to these gates makes the tunnel barriers to the source and drain more opaque. As a result, transport in the few-electron regime, in particular, is difficult to measure. Here, our quasi-1D dot geometry allows us to maintain strong coupling to the leads even in the one- and two-electron regime, as signified by the large (>0.2 e^2/h) Coulomb blockade peaks. In addition, we employed the technique of cooling down the device with the gates at positive bias [14]. This effectively lowers the ionized donor concentration N_{ion} in the vicinity of the dot, and our simulations show that the lowered N_{ion} enhances the spread and lead connectivity of the low lying wave functions.

In Fig. 3 we plot the temperature dependence and in-plane magnetic field dependence of the conductance for the one- and two-electron dot. Our $N = 1$ quantum dot is an experimental realization of the canonical example of the Kondo effect with just a single isolated spin. The Kondo temperature T_K depends sensitively on the coupling to the leads. Figure 3(a) shows that with decreasing temperature, the conductance in the single-electron valley increases, whereas the trend is reversed for the two-electron valley, as expected. Furthermore, we observe that the conductance peaks shift toward the center of the $N = 1$ valley as the temperature is lowered, in agreement with theoretical predictions for the Kondo effect [15]. Applying a parallel magnetic field $B_{\|}$ allows us to measure the Kondo peak splitting [15]. Figure 3(b) shows the differential conductance as a function of V_{SD} and $B_{\|}$ at the center of the $N = 1$ valley. We find that above a critical value of in-plane magnetic field $B_C = 1.45$ T, the Kondo peak begins to split into two peaks located at $eV_{SD} = \pm g\mu_B B_{\|}$, where e is the electron charge, g is the g factor, and μ_B is the Bohr magneton. This splitting allows us to determine the g factor $g = 0.32$ for our quantum dot. The value of the critical magnetic field B_C required for Kondo peak splitting gives us an estimate of the Kondo energy scale $k_B T_K \sim g\mu_B B_C \sim 27$ μeV. A critical magnetic field below which

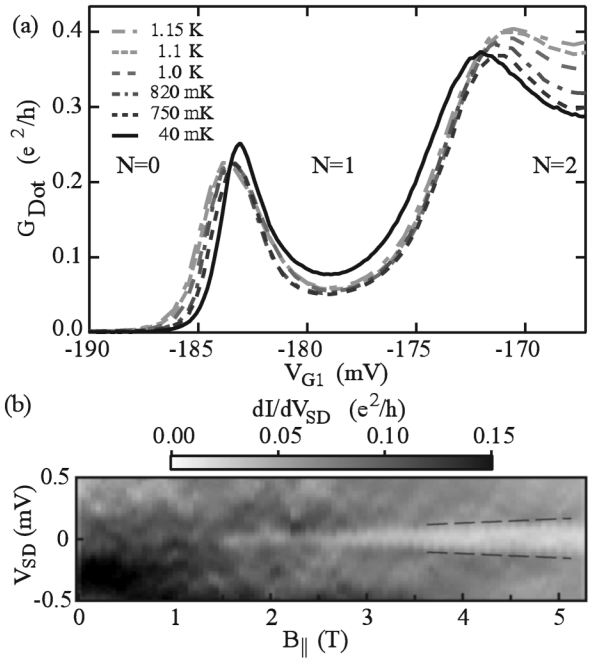

FIG. 3. (a) Conductance versus side gate voltage V_{G1} for different mixing chamber temperatures. (b) Differential conductance as a function of source-drain voltage and in-plane magnetic field (with V_{G1} tuned to the center of the $N = 1$ valley) showing the Kondo peak splitting. Dashed lines are linear fits of the peaks to $\pm g\mu_B B_\parallel$.

no splitting occurs is predicted by theory [16] and has been measured in other lateral quantum dots [17–19].

Figure 4 shows the differential conductance through the quantum dot as a function of V_{SD} and V_{G1} in the one- and two-electron regime. The absence of diamonds at high bias and more negative side gate voltage gives further evidence of the absolute occupancy of the dot ($N = 0$, 1, and 2). The transport spectroscopy shown here has many interesting features. We find several horizontal lines within the Coulomb diamonds. These features form peaks in dI/dV_{SD} rather than steps. This is strong evidence of Kondo behavior, since the Kondo effect relies on tunnel coupling of two (possibly degenerate) states with a Fermi surface or surfaces such that, within the natural level width, the levels have access to both occupied and unoccupied states; i.e., the levels are pinned to the Fermi surface(s). A multipeak Kondo effect where one Fermi surface is pinned to an excited state (and the other to the ground state) has been predicted theoretically [20]. The conductance peaks are found to be nearly parallel with respect to V_{G1}, as expected [20]. To observe multiple Kondo peaks, the Kondo energy $k_B T_K$ should be comparable to or larger than V_{SD}. In our quantum dot, the Kondo energy is expected to be enhanced by the presence of multiple levels in the quantum dot [21].

We begin a closer analysis of Fig. 4 with the $N = 2$ diamond, corresponding to a helium artificial atom. We observe four horizontal peaks in the differential conductance, symmetrically situated, with two peaks above and two peaks below $V_{SD} = 0$. Horizontal features within a Coulomb blockade diamond at a source-drain bias $V_{SD} = \Delta/e$ are associated with transport through an excited state of energy Δ. The four horizontal peaks occur at $\Delta_1 = \pm 105$ μeV and $\Delta_2 = \pm 285$ μeV. We infer that the ground state for the $N = 2$ quantum dot (with $B_\parallel = 0$) is a singlet, because no zero-bias Kondo peak is observed. While the singlet has no Kondo effect, the triplet $S = 1$ typically has a lower T_K than a spin-1/2 system. However, for an even N system it has been demonstrated [8] that near a degeneracy of the singlet and triplet (induced by, say, a magnetic field) a sharp rise of the Kondo temperature results. We therefore propose that the peaks at ± 105 μeV and ± 285 μeV result from the Kondo coupling of the first and second excited-state triplet with the ground state singlet. In other words, the singlet-triplet degeneracy is brought about *modulo* the source-drain bias.

In the $N = 1$ diamond of Fig. 4, we observe several horizontal peaks. In addition to a zero-bias conductance peak, associated with the single-electron Kondo effect, we find additional peaks spaced by roughly 145 μeV. These peaks correspond to the excitation spectrum of the quantum dot. The fabrication of a single-electron dot still appreciably connected to the leads and possessing an excitation spectrum as small as this is nontrivial. The nominal 2DEG density in this heterostructure is $n_s = 3.8 \times 10^{11}$ cm^{-2}. Our modeling shows that with this density of ionized donors and the given geometry of the gates, the gate voltages required to deplete the dot down to one or two

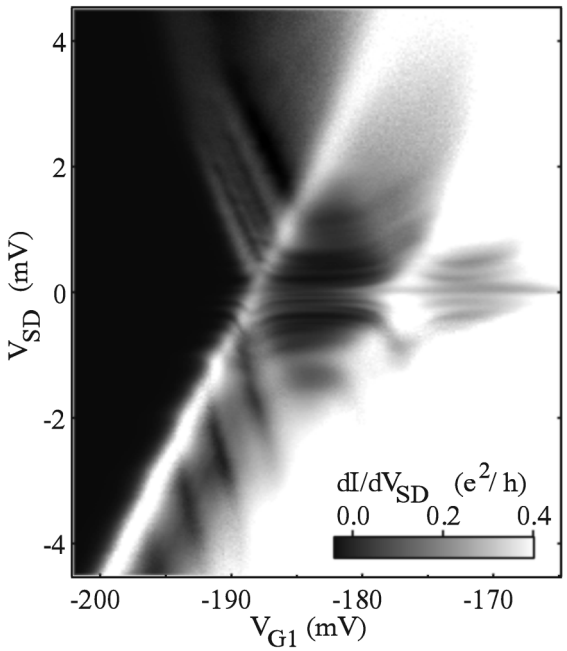

FIG. 4. Differential conductance as a function of source-drain voltage and side gate voltage V_{G1}. Left region is $N = 0$, center diamond is $N = 1$, and right diamond is $N = 2$. Sharp horizontal conductance peaks are observed within the $N = 1$ and $N = 2$ diamonds. Also observed are regions of negative differential conductance above and below the $N = 1$ diamond.

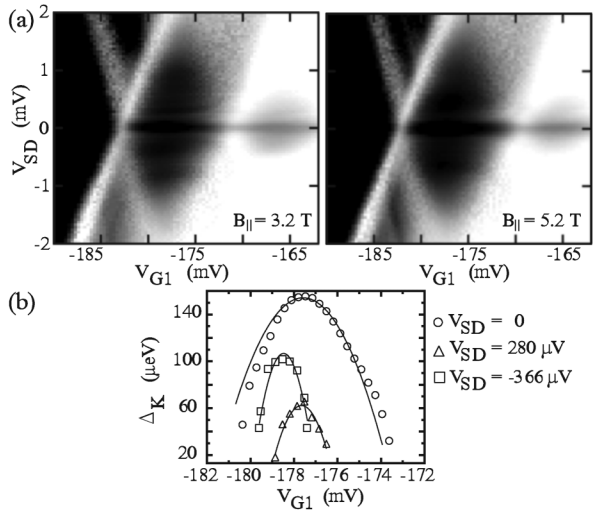

FIG. 5. (a) Differential conductance as a function of source-drain voltage and side gate voltage V_{G1} with (left) $B_{||} = 3.2$ T and (right) $B_{||} = 5.2$ T. Light regions correspond to enhanced conductance. (b) Peak splitting Δ_K, and parabolic fits, for 3 representative peaks at 3.2 T.

electrons would result in a deep, isolated potential depression with a level spacing greater than 1 meV. Therefore, we have artificially reduced the ionized donor density in the region of the dot by cooling the device down with the gates energized at positive bias. Although we cannot measure the resultant local ion density directly, calculating the electronic structure over a range of 1.5×10^{11} cm$^{-2} \geq n_s \geq 0.25 \times 10^{11}$ cm^{-2} results in a level spacing from 500 μeV down to around 200 μeV. The levels are affected by the particular gate voltages and also the addition of discrete donors (as opposed to jellium) to the calculation. While the donor distribution cannot be known for every device with precision, the success of the model in obtaining consistent excitation energies, even in such a low density regime, is significant. We note finally that recent measurements of nonlinear transport in nanowires exhibit comparable ''Kondo stripes'' in the Coulomb blockade diamond and a similar explanation has been considered [22].

Figure 5(a) shows similar data at a parallel magnetic field of 3.2 and 5.2 T. We find that, in addition to the splitting at zero bias, splitting is also found at nonzero bias, roughly at the locations of the peaks at zero magnetic field. Further indication that these peaks are caused by the Kondo effect is found from the peak splitting behavior. It has been predicted [23] that the peak splitting Δ_K, defined as half the separation between the positions of the positive and negative peaks, is proportional to $\log(1/T_K)$. The Kondo temperature T_K varies as $\exp(V_G{}^2)$, where V_G is the side gate voltage [19]. Therefore, the peak splitting Δ_K is expected to vary quadratically with gate voltage. Figure 5(b) shows the peak splitting Δ_K as a function of the side gate voltage for three representative peaks at zero, positive, and negative source-drain bias and $B_{||} = 3.2$ T. We find that the peak splitting does indeed vary quadratically with gate voltage at both zero and finite source-drain bias. The fact that each parabola has a different curvature can be explained by the difference in the energy and tunneling rates of the different quantum dot states.

Our measurements on a small quasi-1D lateral quantum dot strongly coupled to its leads revealed a multi-peak Kondo effect in the one- and two-electron regime. Electronic structure simulations for our dot, which include the full 3D structure of the device, show that the shape of the quantum dot gives rise to low-energy excited states. These excited states are coupled to the leads via a Kondo resonance, giving rise to the observed Kondo stripes within the Coulomb blockade diamonds.

We thank D. Goldhaber-Gordon, J. Martinek, and S. Tarucha for helpful discussions. This work was supported by DARPA-QuIST, the Center for Nanoscale Systems at Harvard University, NNIN/C, and iQUEST at UCSB.

[1] A. C. Hewson, *The Kondo Problem to Heavy Fermions, Cambridge Studies in Magnetism* (Cambridge University Press, Cambridge, England, 1993).
[2] W. J. deHaas, J. H. de Boer, and G. J. van den Berg, Physica (Amsterdam) **1**, 1115 (1934).
[3] L. P. Kouwenhoven *et al.*, in *Mesoscopic Electron Transport*, edited by L. L. Sohn, L. P. Kouwenhoven, and G. Schön (Kluwer, Dordrecht, 1997).
[4] D. Goldhaber-Gordon *et al.*, Nature (London) **391**, 156 (1998); S. M. Cronenwett, T. H. Oosterkamp, and L. P. Kouwenhoven, Science **281**, 540 (1998); J. Schmid *et al.*, Physica (Amsterdam) **256B**, 182 (1998).
[5] F. Simmel *et al.*, Phys. Rev. Lett. **83**, 804 (1999).
[6] S. De Franceschi *et al.*, Phys. Rev. Lett. **89**, 156801 (2002).
[7] J. Schmid *et al.*, Phys. Rev. Lett. **84**, 5824 (2000).
[8] S. Sasaki *et al.*, Nature (London) **405**, 764 (2000).
[9] A. Kogan *et al.*, Phys. Rev. B **67**, 113309 (2003).
[10] S. De Franceschi *et al.*, Phys. Rev. Lett. **86**, 878 (2001).
[11] J. Nygard, D. H. Cobden, and P. E. Lindelof, Nature (London) **408**, 342 (2000).
[12] L. Wang, J. K. Zhang, and A. R. Bishop, Phys. Rev. Lett. **73**, 585 (1994).
[13] M. Field *et al.*, Phys. Rev. Lett. **70**, 1311 (1993).
[14] M. Pioro-Ladrière *et al.*, Phys. Rev. B **72**, 115331 (2005).
[15] Y. Meir, N. S. Wingreen, and P. A. Lee, Phys. Rev. Lett. **70**, 2601 (1993); N. S. Wingreen and Y. Meir, Phys. Rev. B **49**, 11 040 (1994).
[16] T. A. Costi, Phys. Rev. Lett. **85**, 1504 (2000).
[17] A. Kogan *et al.*, Phys. Rev. Lett. **93**, 166602 (2004).
[18] D. M. Zumbuhl *et al.*, Phys. Rev. Lett. **93**, 256801 (2004).
[19] S. Amasha *et al.*, Phys. Rev. B **72**, 045308 (2005).
[20] T. Inoshita *et al.*, Phys. Rev. B **48**, R14725 (1993); Superlattices Microstruct. **22**, 75 (1997).
[21] With $k_B T_K$ of 27 μeV as our single level Kondo energy, and a single additional level at 145 μeV, we obtain using Eq. (3) in Ref. [20] an enhanced $k_B T_K$ equal to 300 μeV.
[22] C. M. Lieber (private communication).
[23] J. E. Moore and X.-G. Wen, Phys. Rev. Lett. **85**, 1722 (2000).